

LETTERS

Isotopic evidence for Mesoarchaeoan anoxia and changing atmospheric sulphur chemistry

James Farquhar¹, Marc Peters², David T. Johnston¹, Harald Strauss², Andrew Masterson¹, Uwe Wiechert³ & Alan J. Kaufman¹

The evolution of the Earth's atmosphere is marked by a transition from an early atmosphere with very low oxygen content to one with an oxygen content within a few per cent of the present atmospheric level. Placing time constraints on this transition is of interest because it identifies the time when oxidative weathering became efficient, when ocean chemistry was transformed by delivery of oxygen and sulphate, and when a large part of Earth's ecology changed from anaerobic to aerobic¹. The observation of non-mass-dependent sulphur isotope ratios in sedimentary rocks more than ~2.45 billion years (2.45 Gyr) old and the disappearance of this signal in younger sediments is taken as one of the strongest lines of evidence for the transition from an anoxic to an oxic atmosphere around 2.45 Gyr ago^{1–5}. Detailed examination of the sulphur isotope record before 2.45 Gyr ago also reveals early and late periods of large amplitude non-mass-dependent signals bracketing an intervening period when the signal was attenuated^{5–9}. Until recently, this record has been too sparse to allow interpretation, but collection of new data has prompted some workers⁸ to argue that the Mesoarchaeoan interval (3.2–2.8 Gyr ago) lacks a non-mass-dependent signal, and records the effects of earlier and possibly permanent oxygenation of the Earth's atmosphere. Here we focus on the Mesoarchaeoan interval, and demonstrate preservation of a non-mass-dependent signal that differs from that of preceding and following periods in the Archaean. Our findings point to the persistence of an anoxic early atmosphere, and identify variability within the isotope record that suggests changes in pre-2.45-Gyr-ago atmospheric pathways for non-mass-dependent chemistry and in the ultraviolet transparency of an evolving early atmosphere.

The report seven years ago of non-mass-dependent isotope signals in a global distribution of Archaean and early Palaeoproterozoic sediments and metasediments⁵ prompted a focused effort to understand the connections between the early sulphur cycle and the history of atmospheric oxygen. These non-mass-dependent effects do not follow the mass-dependent relationships $\delta^{33}\text{S} \approx 0.5\delta^{34}\text{S}$ and $\delta^{36}\text{S} \approx 2\delta^{34}\text{S}$, where the terms 0.5 and 2 reflect the relative mass differences between the numerator and denominator of $^{33}\text{S}/^{32}\text{S}$ and $^{36}\text{S}/^{32}\text{S}$ compared to those of $^{34}\text{S}/^{32}\text{S}$ (see Methods for definitions of notation and a more detailed description of non-mass-dependent and mass-dependent isotope effects). Work on this topic has yielded a growing data set of $\Delta^{33}\text{S}$ and $\Delta^{36}\text{S}$ (a measure of the deviation from a reference array that approximates low temperature chemical equilibrium and passes through bulk Earth composition; see Methods) that is fully complementary to the existing $\delta^{34}\text{S}$ data and interpretations made from this time series record. These data ($\delta^{34}\text{S}$, $\Delta^{33}\text{S}$ and $\Delta^{36}\text{S}$) provide new insights into the processes and conditions necessary to produce

non-mass-dependent sulphur isotope effects in the Archaean and earliest Palaeoproterozoic, as well as into the post-2.45-Gyr-ago world, where mass-dependent isotope effects are preserved^{7,10–12}, and non-mass-dependent effects are largely absent—the exception being effects reported for some atmospheric samples and accumulations in ice cores^{13–15}.

Figure 1 illustrates the dramatic change in the magnitude of $\Delta^{33}\text{S}$ that occurred between ~2.45 and 2.32 Gyr ago^{1,6,12}. The disappearance of large $\Delta^{33}\text{S}$ in the rocks younger than ~2.45 Gyr reflects the suppression of the non-mass-dependent effects. Concomitant enhancement of mass-dependent signals (brought about by significantly larger sources of sulphate sulphur from oxidative weathering) reflects a shift from a sulphur cycle conducive to preservation of atmospheric isotope effects to a sulphur cycle in which biological isotope effects dominate. A corresponding increase in the range of $\delta^{34}\text{S}$ (Fig. 2) has been attributed to the more significant role for sulphate reducing microorganisms in oceanic environments with higher sulphate concentrations. This figure also illustrates temporal variations in the Archaean $\Delta^{33}\text{S}$ record, including an apparent

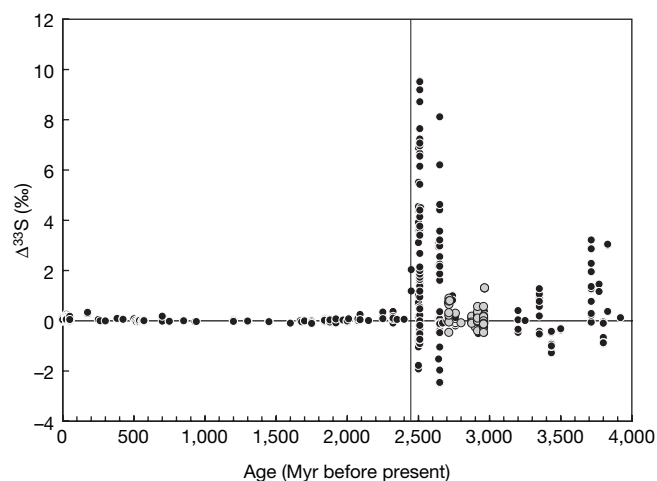


Figure 1 | Compilation of $\Delta^{33}\text{S}$ versus age for rock samples. Data are taken from refs 5–8, 12, 19–30. Ion probe data have been grouped by sample averages when measurements of different grains in the same sample did not vary outside reported uncertainties. The figure illustrates large $\Delta^{33}\text{S}$ before ~2.45 Gyr ago (indicated by vertical line), and small but measurable $\Delta^{33}\text{S}$ after 2.45 Gyr ago. Detailed examination of the pre-2.45-Gyr-ago record indicates an apparent minimum for $\Delta^{33}\text{S}$ during the Mesoarchaeoan (2.8–3.2 Gyr ago). Uncertainties are smaller than the symbol sizes for $\Delta^{33}\text{S}$. Filled black circles are data from literature; filled grey circles are data presented in this study.

¹Department of Geology and ESSIC, University of Maryland, College Park, Maryland 20742, USA. ²Geologisch-Paläontologisches Institut und Museum der Westfälischen Wilhelms-Universität Münster, Corrensstraße 24, 48149 Münster, Germany. ³Department of Earth Sciences, Freie Universität Berlin, Maltesserstr. 74-100, Haus B, C und N, 12249 Berlin, Germany.

minimum in the absolute range of $\Delta^{33}\text{S}$ in the Mesoarchaeon (published and new data are presented in Supplementary Table 1). A question raised by the data, and one we focus on here, is whether this minimum reflects an absence of processes that produce non-mass-dependent fractionations⁸, or whether it reflects something that caused the amplitude of $\Delta^{33}\text{S}$ to diminish, but did not turn off non-mass-dependent processes. The answer to this question rests with the cause and character of the non-mass-dependent effects.

The reports of non-mass-dependent sulphur isotope signals in modern atmospheric sulphate aerosols¹³, and in sulphate produced from volcanogenic SO_2 recovered from horizons in Antarctic ice cores and firn^{14,15}, have been attributed to stratospheric reactions involving SO_2 , and provide one link to the atmosphere^{13–15}. Additional links to the atmosphere have been made on the basis of photolysis experiments with SO_2 , a species inferred to be present in the atmosphere throughout Earth history. These experiments yield large non-mass-dependent isotope effects that exhibit a dependence on wavelength and are similar in many respects to the sulphur isotope compositions observed in the geologic record².

The connection to these photolysis experiments and to modern stratospheric chemistry is taken as evidence that the early atmosphere was (partially or wholly) transparent to deep ultraviolet radiation—to allow similar chemical reactions to occur. An atmosphere transparent to deep ultraviolet would imply a low column depth for ozone, and also for oxygen because ozone is maintained at present high levels by chemistry involving atmospheric oxygen. Models of atmospheric chemistry imply a second connection to oxygen concentrations in the atmosphere. This is because the pathways for the transfer of non-mass-dependent sulphur to Earth's surface as aerosols (S_8 and sulphate) depend on whether oxygen and other oxygen species were high enough to consume neutral sulphur species (for example, S , S_2 and S_3)³. In low oxygen conditions, S_8 aerosols are stabilized in addition to sulphate aerosols and this allows for a more efficient

transfer of atmospheric non-mass-dependent signals to surface sulphur and sulphate pools.

To investigate further the possibility of a non-mass-dependent effect in the Mesoarchaeon (and slightly post-Mesoarchaeon) record, we illustrate the covariation of $\delta^{34}\text{S}$ with $\Delta^{33}\text{S}$ for Mesoarchaeon samples (Fig. 2), which provides a means to explore the significance of the attenuated $\Delta^{33}\text{S}$ in this interval. Although the absolute magnitude of the $\Delta^{33}\text{S}$ effect for these samples is smaller than observed in other portions of the Archaean (and in particular, the earliest Palaeoproterozoic), the $\delta^{34}\text{S}$ versus $\Delta^{33}\text{S}$ field is entirely consistent with the overall field for the Archaean/earliest Palaeoproterozoic data; it is also distinct from samples younger than 2.45 Gyr when the atmosphere was undeniably oxidized. We include data presented by Ohmoto *et al.*⁸ and Ono *et al.*⁷ in Fig. 2 to illustrate the striking consistency of each existing set of Mesoarchaeon data with the non-mass-dependent (or pre-2.45-Gyr ago) array rather than the mass-dependent (or post-2.45-Gyr ago) array.

Although the non-mass-dependent signal may have been attenuated during the Mesoarchaeon, our compilation illustrates a larger range of $\Delta^{33}\text{S}$ variation than observed by Ohmoto *et al.*⁸ and further suggests active non-mass-dependent chemistry. To support this contention, we provide an additional (and established) metric for distinguishing non-mass-dependent from mass-dependent signals with the concurrent measurement of ^{36}S abundances and the construction of $\Delta^{36}\text{S}/\Delta^{33}\text{S}$ arrays (Fig. 3)^{5,7}. The low $\Delta^{36}\text{S}$ values in Fig. 3a reflect Rayleigh amplification of mass-dependent fractionation effects and define the limits of the mass-dependent field; they are well explained by theoretical considerations¹⁶. Covariation of $\Delta^{36}\text{S}$ with $\Delta^{33}\text{S}$ forms one of the principal arguments for a gas-phase photolytic origin of the effects observed in the Archaean/earliest Palaeoproterozoic record, and mass-dependent samples define a restricted field on a plot of $\Delta^{36}\text{S}$ versus $\Delta^{33}\text{S}$ that is distinct from the field defined by Archaean/earliest Palaeoproterozoic samples.

The Mesoarchaeon data from this study, and one data point previously suggested to be anomalous by Ono *et al.*⁷, define fields that are distinct from the greater Archaean data set and the mass-dependent post-2.45-Gyr intervals. The differences between the Mesoarchaeon data set and the data set for older Archaean samples are inconsistent with a non-mass-dependent signal that was inherited from pre-existing terranes, and support the view of a pervasive anoxic atmosphere throughout the Archaean eon and into the earliest Palaeoproterozoic. Although some Mesoarchaeon samples (for example, from the Nsuzi, Moodies and Mozaan⁷ Groups) overlap the mass-dependent array for $\Delta^{36}\text{S}/\Delta^{33}\text{S}$, evidence for the large $\delta^{34}\text{S}$ range that is required to produce these minor isotope variations by mass-dependent processes (see, for example, ref. 16) is not observed in samples from this time interval. We also point out that the Mesoarchaeon data form distinct fields when grouped at the formation level (Fig. 3b), illustrating fundamental changes in Mesoarchaeon non-mass-dependent signals, and we highlight similarities in the Mesoarchaeon signals from sequences in South Africa and those in Western Australia.

Insight into the origin of the Mesoarchaeon isotope variation (a diminished $\Delta^{33}\text{S}$ amplitude and variable $\Delta^{36}\text{S}/\Delta^{33}\text{S}$) is provided by considering results from photochemical experiments and by comparisons with other Archaean intervals. The $\delta^{34}\text{S}$, $\Delta^{33}\text{S}$ and $\Delta^{36}\text{S}$ variations for some parts of the Archaean record—for example, the ~3.4-Gyr-old successions in Western Australia and South Africa—appear to be well-matched by experiments undertaken with ~193 nm radiation², and this observation led to the suggestion that deep-ultraviolet photolysis of sulphur dioxide provided an explanation for the origin of the non-mass-dependent signal in the Archaean eon. A subsequent study⁶ documented a different relationship for $\delta^{34}\text{S}$ and $\Delta^{33}\text{S}$ variations (for the ~2.5-Gyr-old Mt McRae Shale), which fell between arrays produced by photolysis at 193 nm and experiments undertaken at longer wavelengths¹⁷; this led to a revised explanation for the non-mass-dependent signal—that it reflects a

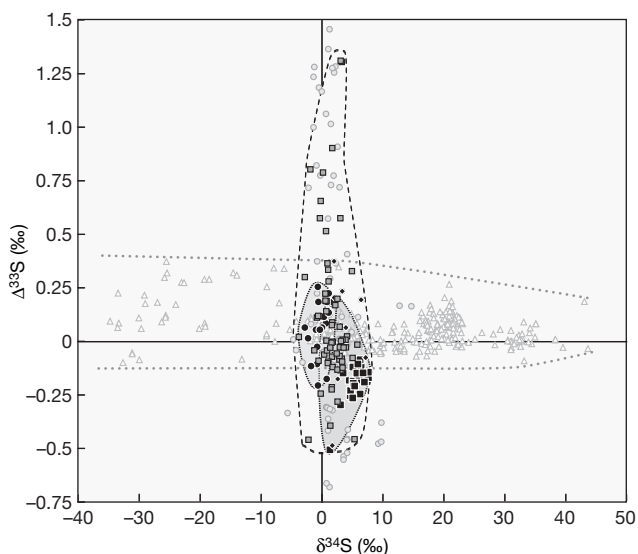
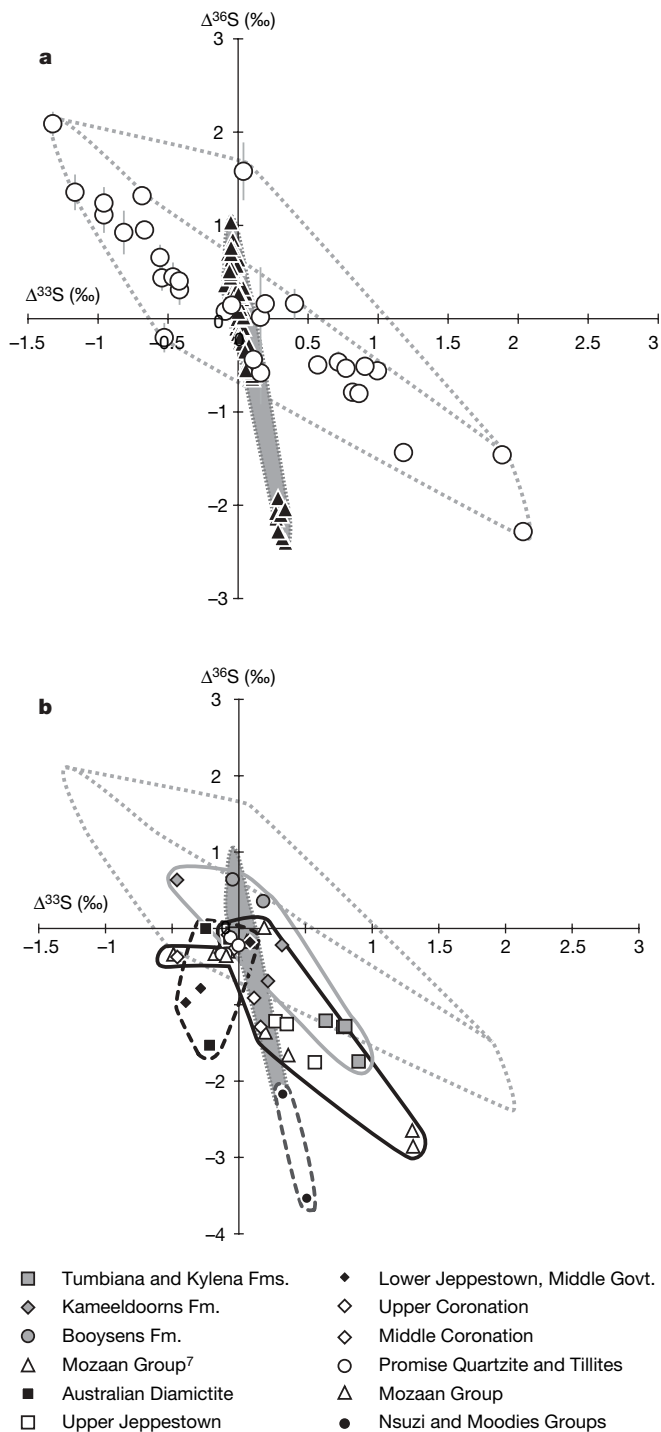


Figure 2 | Plot of $\Delta^{33}\text{S}$ versus $\delta^{34}\text{S}$ that illustrates the fields defined by pre- and post-2.45-Gyr-ago samples. The dotted grey line marks the limits of the observed post-2.45-Gyr-ago field. Fields are also included for published data, including samples from the Mozaan group⁷ (filled black diamonds), samples from the Hardey Formation⁸ (filled black circles), samples from the Mosquito Creek Formation⁸ (filled black squares), and data from this study (filled grey squares). The field for the data from this study is outlined with a dashed black outline, as are the fields for literature data for the Hardey Formation, the Mosquito Creek Formation and the Mozaan Group, which are outlined with dotted black outlines and also shaded in grey. Grey unfilled triangles are literature data for post 2.45-Gyr-ago samples and grey filled circles are literature data for pre 2.45-Gyr-ago samples, excluding those listed above. Uncertainties for the data presented in this study are smaller than the symbol sizes for $\Delta^{33}\text{S}$ and $\delta^{34}\text{S}$.



combination of effects produced at shorter and longer ultraviolet wavelengths^{6,18}. The data for the Mesoarchaeon produce another relationship between $\delta^{34}\text{S}$, $\Delta^{33}\text{S}$ and $\Delta^{36}\text{S}$ that adds complexity but may also provide a way to reconcile the observations made of Palaeoarchean² and Neoarchaeon⁶ samples if they reflect changes in the source reactions that occurred through Archaean time.

The photolysis experiments^{2,18} exhibit a wavelength dependence that can account for the observed $\delta^{34}\text{S}$, $\Delta^{33}\text{S}$ and $\Delta^{36}\text{S}$ relationships, and we speculate that changing transparency of the atmosphere may account for the observed minor sulphur isotope variation across the Archaean eon. In this context, the presence of variability for the Mesoarchaeon data on plots of the $\Delta^{36}\text{S}$ versus $\Delta^{33}\text{S}$ (Fig. 3b) may also signal changes in atmospheric sulphur chemistry or transport. It is not clear whether the distinct arrays for samples grouped at

Figure 3 | Plot of $\Delta^{36}\text{S}$ versus $\Delta^{33}\text{S}$ for mass-dependent and mass-independent data. **a**, Plot of $\Delta^{36}\text{S}$ versus $\Delta^{33}\text{S}$ for pre-2.45-Gyr-ago samples (circles)⁵ and for mass-dependent data (triangles)^{16,19,20} (note that we have not included data from ref. 5 in the mass-dependent data set because of concerns about the exponent for $\Delta^{36}\text{S}$ noted in ref. 21). **b**, Plot of $\Delta^{36}\text{S}$ versus $\Delta^{33}\text{S}$ for samples reported in this study and by Ono *et al.*⁷. The field defined by the Archaean/earliest Palaeoproterozoic samples is outlined by a dotted line, and the field defined by the mass-dependent samples is outlined by a dotted line and shaded light grey. Data grouped into the field outlined by the solid grey line include data from the Kameeldoorns Formation (filled grey diamonds), the Tumbiana and Kylenea Formations (filled grey squares) and the Booyens Formation (filled grey circles). Data grouped into the field outlined by a solid black line includes the Mozaan Group (unfilled triangles), the Upper Jeppestown Formation (unfilled squares), the Middle and Upper Coronation Shale (unfilled diamonds) and the Promise Quartzite and Tillites (unfilled circles). Data for the Lower Jeppestown and Middle Government subgroup (filled black diamonds) and from the basal Fortescue group associated with diamictites (filled black squares) are grouped separately in a field surrounded by a dashed black line, and data for samples from the Nsuzi Group and the Moodies Group (filled black circles) are in a field outlined by a dashed grey line. Uncertainties for $\Delta^{33}\text{S}$ are smaller than the symbol size, and uncertainties for $\Delta^{36}\text{S}$ are twice the symbol size.

the formation level within the Mesoarchaeon indicate that the non-mass-dependent reactions tell us about specific states of the atmosphere, but we suggest that the fanning of these arrays rather than a coherence from formation to formation points to a control that varies on timescales represented by the formations themselves. Our data therefore point to continued low oxygen conditions throughout the Archaean, and imply changes in chemistry. These changes might be related to variations in the relative abundance of trace gas species (maybe SO_2), or to fluctuations in ultraviolet radiation transmitted through the atmosphere. Such fluctuations could reflect changes in atmospheric composition or the formation of atmospheric organic aerosol hazes.

METHODS SUMMARY

Sulphur isotope analyses were undertaken using standard fluorination methods and dual inlet gas-source mass spectrometry of sulphur extracted from samples by standard techniques (see Methods for details). Sulphur isotope ratios were measured for SF_6 as the analyte using a ThermoFinnigan MAT 253. The data are described using standard notation: $\delta^{34}\text{S} = 1,000 \times ((^{34}\text{S}/^{32}\text{S})_{\text{sample}} / (^{34}\text{S}/^{32}\text{S})_{\text{ref}} - 1)$, $\Delta^{33}\text{S} = 1,000 \times ((^{33}\text{S}/^{32}\text{S})_{\text{sample}} / (^{33}\text{S}/^{32}\text{S})_{\text{ref}} - ((^{34}\text{S}/^{32}\text{S})_{\text{sample}} / (^{34}\text{S}/^{32}\text{S})_{\text{ref}})^{0.515})$, and $\Delta^{36}\text{S} = 1,000 \times ((^{36}\text{S}/^{32}\text{S})_{\text{sample}} / (^{36}\text{S}/^{32}\text{S})_{\text{ref}} - ((^{34}\text{S}/^{32}\text{S})_{\text{sample}} / (^{34}\text{S}/^{32}\text{S})_{\text{ref}})^{1.9})$.

Full Methods and any associated references are available in the online version of the paper at www.nature.com/nature.

Received 8 March; accepted 14 August 2007.

- Holland, H. D. The oxygenation of the atmosphere and oceans. *Phil. Trans. R. Soc. B* 361, 903–915 (2006).
- Farquhar, J., Savarino, J., Airieau, S. & Thiemens, M. H. Observation of wavelength-sensitive mass-independent sulfur isotope effects during SO_2 photolysis: Implications for the early atmosphere. *J. Geophys. Res.* E 106, 32829–32839 (2001).
- Pavlov, A. A. & Kasting, J. F. Mass-independent fractionation of sulfur isotopes in Archean sediments: Strong evidence for an anoxic Archean atmosphere. *Astrobiology* 2, 27–41 (2002).
- Zahnle, K., Claire, M. & Catling, D. The loss of mass-independent fractionation in sulfur due to a Palaeoproterozoic collapse of atmospheric methane. *Geobiology* 4, 271–283 (2006).
- Farquhar, J., Bao, H. & Thiemens, M. Atmospheric influence of Earth's earliest sulfur cycle. *Science* 289, 756–758 (2000).
- Ono, S. *et al.* New insights into Archean sulfur cycle from mass-independent sulfur isotope records from the Hamersley Basin, Australia. *Earth Planet. Sci. Lett.* 213, 15–30 (2003).
- Ono, S., Beukes, N. J., Rumble, D. & Fogel, M. L. Early evolution of atmospheric oxygen from multiple sulfur and carbon isotope records of the 2.9 Ga Mozaan Group of the Pongola Supergroup, Southern Africa. *South Afr. J. Geol.* 109, 97–108 (2006).
- Ohmoto, H., Watanabe, Y., Ikemi, H., Poulson, S. R. & Taylor, B. E. Sulphur isotope evidence for an oxic Archean atmosphere. *Nature* 442, 908–911 (2006).
- Kasting, J. F. & Ono, S. Palaeoclimates: the first two billion years. *Phil. Trans. R. Soc. B* 361, 917–929 (2006).

10. Farquhar, J. *et al.* Multiple sulfur isotopic interpretations of biosynthetic pathways. *Geobiology* **1**, 27–36 (2003).
11. Johnston, D. T. *et al.* Active microbial sulfur disproportionation in the Mesoproterozoic. *Science* **310**, 1477–1479 (2005).
12. Bekker, A. *et al.* Dating the rise of atmospheric oxygen. *Nature* **427**, 117–120 (2003).
13. Romero, A. B. & Thieme, M. H. Mass-independent sulfur isotopic compositions in present-day sulfate aerosols. *J. Geophys. Res.* **D 108**, doi:10.1029/2003JD003660 (2003).
14. Savarino, J., Romero, A., Cole-Dai, J., Bekki, S. & Thieme, M. H. UV induced mass-independent sulfur isotope fractionation in stratospheric volcanic sulfate. *Geophys. Res. Lett.* **30**, doi:10.1029/2003GL018134 (2003).
15. Baroni, M., Thieme, M. H., Delmas, R. J. & Savarino, J. Mass-independent sulfur isotopic compositions in stratospheric volcanic eruptions. *Science* **315**, 84–87 (2007).
16. Ono, S., Wing, B., Johnston, D., Farquhar, J. & Rumble, D. Mass-dependent fractionation of quadruple stable sulfur isotope system as a new tracer of sulfur biogeochemical cycles. *Geochim. Cosmochim. Acta* **70**, 2238–2252 (2006).
17. Farquhar, J. & Wing, B. A. Multiple sulfur isotopes and the evolution of the atmosphere. *Earth Planet. Sci. Lett.* **213**, 1–13 (2003).
18. Farquhar, J., Savarino, J., Jackson, T. L. & Thieme, M. H. Evidence of atmospheric sulphur in the martian regolith from sulphur isotopes in meteorites. *Nature* **404**, 50–52 (2000).
19. Ono, S., Shanks, W. C., Rouxel, O. J. & Rumble, D. ³³S constraints on the seawater sulfate contribution in modern seafloor hydrothermal vent sulfides. *Geochim. Cosmochim. Acta* **71**, 1170–1182 (2007).
20. Johnston, D. T. *et al.* Evolution of the oceanic sulfur cycle at the end of the Paleoproterozoic. *Geochim. Cosmochim. Acta* **70**, 5723–5739 (2006).
21. Farquhar, J., Bao, H. M., Thieme, M. H., Hu, G. X. & Rumble, D. Questions regarding Precambrian sulfur isotope fractionation — Response. *Science* **292**, U6–U7 (2001).
22. Farquhar, J. & Wing, B. A. in *Mineral Deposits and Earth Evolution* (eds McDonald, I., Boyce, A. J., Butler, I. B., Herrington, R. J. & Polya, D. A.) 167–177 (Spec. Publ. 248, Geological Society, London, 2005).
23. Whitehouse, M. J. *et al.* Integrated Pb- and S-isotope investigation of sulphide minerals from the early Archaean of southwest Greenland. *Chem. Geol.* **222**, 112–131 (2005).
24. Papineau, D., Mojzsis, S. J., Coath, C. D., Karhu, J. A. & McKeegan, K. D. Multiple sulfur isotopes of sulfides from sediments in the aftermath of Paleoproterozoic glaciations. *Geochim. Cosmochim. Acta* **69**, 5033–5060 (2005).
25. Mojzsis, S. J., Coath, C. D., Greenwood, J. P., McKeegan, K. D. & Harrison, T. M. Mass-independent isotope effects in Archean (2.5 to 3.8 Ga) sedimentary sulfides determined by ion microprobe analysis. *Geochim. Cosmochim. Acta* **67**, 1635–1658 (2003).
26. Hu, G. X., Rumble, D. & Wang, P. L. An ultraviolet laser microprobe for the in situ analysis of multisulfur isotopes and its use in measuring Archean sulfur isotope mass-independent anomalies. *Geochim. Cosmochim. Acta* **67**, 3101–3118 (2003).
27. Ono, S., Wing, B., Johnston, D., Farquhar, J. & Rumble, D. Mass-dependent fractionation of quadruple stable sulfur isotope system as a new tracer of sulfur biogeochemical cycles. *Geochim. Cosmochim. Acta* **70**, 2238–2252 (2006).
28. Cates, N. L. & Mojzsis, S. J. Chemical and isotopic evidence for widespread Eoarchean metasedimentary enclaves in southern West Greenland. *Geochim. Cosmochim. Acta* **70**, 4229–4257 (2006).
29. Papineau, D. & Mojzsis, S. J. Mass-independent fractionation of sulfur isotopes in sulfides from the pre-3770 Ma Isua Supracrustal Belt, West Greenland. *Geobiology* **4**, 227–238 (2006).
30. Kamber, B. S. & Whitehouse, M. J. Micro-scale sulphur isotope evidence for sulphur cycling in the late Archean shallow ocean. *Geobiology* **5**, 5–17 (2007).

Supplementary Information is linked to the online version of the paper at www.nature.com/nature.

Acknowledgements This study was supported by funds from the NSF EAR, NASA NAI and NASA EXB programmes (to J.F.), and revisions were undertaken while J.F. was supported by a visiting appointment at the IPG of Paris. Other support for this work came from NSF (A.J.K.) and the DFG (H.S.). The manuscript was improved by reviews and comments from P. Knauth and H. Ohmoto. P. Cartigny is thanked for reading and commenting on the manuscript.

Author Information Reprints and permissions information is available at www.nature.com/reprints. Correspondence and requests for materials should be addressed to J.F. (jfarquha@geol.umd.edu).

METHODS

We use a framework for distinguishing non-mass-dependent and mass-dependent isotope effects made using data collected from the geologic record that is anchored in an understanding of the way that mass-dependent processes operate. Our framework is distinct from those that place the distinction between non-mass-dependent and mass-dependent fractionations using only a threshold of $\Delta^{33}\text{S}$ (for example, at $\sim 0.4\%$; ref. 31) because it also considers information present in correlations between $\delta^{34}\text{S}$, $\Delta^{33}\text{S}$ and $\Delta^{36}\text{S}$. While this provides a more robust test of the presence of non-mass-dependent effects, we recognize that there will be an overlap in the fields for mass-dependent and non-mass-dependent signals. In some cases, samples that belong to non-mass-dependent populations may overlap with the range of the mass-dependent population.

In this study, sulphur from 66 samples were extracted using chromium reduction and converted to silver sulphide, converted to SF_6 by fluorination in a Ni reaction vessel at 250°C with $\sim 10\times$ excess F_2 gas, and then purified by cryogenic and chromatographic techniques as described elsewhere³². Isotope ratios were determined by dual inlet IRMS using a ThermoFinnigan MAT 253 mass spectrometer with simultaneous monitoring of 127, 128, 129 and 131 (AMU/e^-). Uncertainties on mass-dependent reference materials are better than $\pm 0.2\%$, $\pm 0.01\%$ and $\pm 0.2\%$ in $\delta^{34}\text{S}$, $\Delta^{33}\text{S}$ and $\Delta^{36}\text{S}$, respectively. Uncertainties on the measurements reported here are estimated to be better than 0.2% , $\pm 0.02\%$ and $\pm 0.2\%$. The results of our measurements are presented in Supplementary Table 1 and in Figs 1, 2 and 3.

Mass-dependent and non-mass-dependent fractionation. Geological interpretation of the sulphur isotope record has benefited significantly from the context provided by an understanding of the mechanisms that produce mass-dependent and non-mass-dependent isotopic fractionations. Mass-dependent fractionation effects arise when variations in chemical and physical properties of isotopologous species depend on the relative differences in mass of the atoms in a molecule, or the mass of the molecular species itself. Mass-dependent fractionations include, but are not limited to, equilibrium isotope exchange, diffusion, gravitational separation and biological effects^{32–36}. Non-mass-dependent fractionations arise when variations in chemical and physical properties of molecular species depend on factors other than or in addition to the mass of the constituent isotopes^{37–39}. Non-mass-dependent fractionations include those associated with symmetry changes of molecular species that arise from a particular isotope substitution, effects associated with internal conversions and intersystem crossings between bound and unbound states, effects associated with nuclear and electronic spin coupling, effects associated with self or mutual shielding, and effects that result from the physical production or destruction of an isotope. It has been established that non-mass-dependent and mass-dependent effects can occur together during chemical reactions or physical processes. For the purposes of this discussion, we will discuss non-mass-dependent effects as those that produce large deviations from mass-dependent fractionation arrays and involve factors other than mass, and we therefore do not include effects associated with mixing of different pools that are fractionated by mass-dependent processes. Our mass-dependent reference array is defined both by model predictions that take into consideration chemical and kinetic mass-dependent reactions and also by observations from oceanic sedimentary rocks. For this comparison, we have not included analyses of reagents or of samples of unknown provenance or age reported in refs 39 or 40.

We interpret the sulphur isotope data presented in Ohmoto *et al.*³¹ to indicate that primary non-mass-dependent chemical effects were part of the sulphur cycles during deposition of the 2.76-Gyr-old Hardey Formation and the 2.92-Gyr-old Mosquito Creek Formation. These workers suggested that the signal observed in the rock record between 2.8 and 3.0 Gyr ago may reflect alternative processes, such as (1) high altitude chemistry involving sulphur dioxide photochemistry, (2) Rayleigh amplification of mass-dependent effects such as those that occur at fractionation crossovers, or (3) non-mass-dependent chemical reactions associated with the sulphate reduction reactions by amino acids. The first possibility has been discussed in ref. 41 and considered unlikely, considering

the distribution of volcanogenic sulphur in the atmosphere and constraints imposed by models of volcanic plume ascent, and the second suggestion can be ruled out on the basis of relationships between $\Delta^{33}\text{S}$ and $\Delta^{36}\text{S}$ that do not form a single array as is expected for Rayleigh amplification of a mass-dependent process, even one occurring at fractionation crossovers. The third suggestion remains to be demonstrated in a form that can be evaluated in the context of the emerging record of the four sulphur isotopes that includes evidence for systematic changes of $\Delta^{36}\text{S}/\Delta^{33}\text{S}$, and possibly of systematic changes in the magnitude of the $\Delta^{33}\text{S}$ and the relationship between $\delta^{34}\text{S}$ and $\Delta^{33}\text{S}$. The viability of alternative hypotheses must be demonstrated to be consistent with the $\Delta^{36}\text{S}/\Delta^{33}\text{S}$ and $\delta^{34}\text{S}/\Delta^{33}\text{S}$. It also should account for any other observations in the record, including the possibility that there may be basinal and global correlations in the record and systematic variations in the relationships between these various measures of sulphur isotope composition.

Our conclusion primarily differs from those in Ohmoto *et al.*³¹ because we have included constraints implied by the $\delta^{34}\text{S}$ data, which was not used to make the assertions in Ohmoto *et al.*³¹. This evaluation can be tested further using $\Delta^{36}\text{S}$ and the relationships between $\Delta^{36}\text{S}$ and $\Delta^{33}\text{S}$. For instance, it is possible that some of the $\Delta^{36}\text{S}/\Delta^{33}\text{S}$ variation in the Archaean data set may reflect the convolution of a mass-dependent signal with a non-mass-dependent signal of Archaean origin, and this possibly accounts for the variation in the $\Delta^{36}\text{S}$ at $\Delta^{33}\text{S} = 0$ for the larger Archaean data set, but this explanation does not account for the full magnitude of the $\Delta^{36}\text{S}$ variability in the Mesoproterozoic and changes in $\Delta^{36}\text{S}/\Delta^{33}\text{S}$. We also recognize the possibility that processes other than photochemistry may contribute to the signals that are observed, but note that experimental evidence for non-mass-dependent effects involving gases of volcanogenic origin in combination with constraints from chemical models of anoxic atmospheres anticipates these effects in Earth's earliest anoxic environments. A subtle, but important point here is that the sulphur signal cannot be simply be an inherited detrital component if it has a different multiple sulphur isotope character, and even if there are detrital components, an authigenic Mesoproterozoic component is inferred. An unresolved aspect of this signal in the Archaean sections is the observation of larger non-mass-dependent signals in shales, banded iron formations, and barites when compared to coarser clastic sediments.

- Ohmoto, H., Watanabe, Y., Ikemi, H., Poulson, S. R. & Taylor, B. E. Sulphur isotope evidence for an oxic Archaean atmosphere. *Nature* **442**, 908–911 (2006).
- Johnston, D. T. *et al.* Evolution of the oceanic sulfur cycle at the end of the Paleoproterozoic. *Geochim. Cosmochim. Acta* **70**, 5723–5739 (2006).
- Farquhar, J. *et al.* Multiple sulfur isotopic interpretations of biosynthetic pathways. *Geobiology* **1**, 27–36 (2003).
- Johnston, D. T. *et al.* Active microbial sulfur disproportionation in the Mesoproterozoic. *Science* **310**, 1477–1479 (2005).
- Ono, S., Shanks, W. C., Rouxel, O. J. & Rumble, D. ^{33}S constraints on the seawater sulfate contribution in modern seafloor hydrothermal vent sulfides. *Geochim. Cosmochim. Acta* **71**, 1170–1182 (2007).
- Farquhar, J. & Wing, B. A. Multiple sulfur isotopes and the evolution of the atmosphere. *Earth Planet. Sci. Lett.* **213**, 1–13 (2003).
- Thiemens, M. H. Atmosphere science — Mass-independent isotope effects in planetary atmospheres and the early solar system. *Science* **283**, 341–345 (1999).
- Thiemens, M. H. History and applications of mass-independent isotope effects. *Annu. Rev. Earth Planet. Sci.* **34**, 217–262 (2006).
- Hulston, J. R. & Thodem, H. G. Variations in ^{33}S , ^{34}S and ^{36}S contents of meteorites and their relation to chemical and nuclear effects. *J. Geophys. Res.* **70**, 3475–3484 (1965).
- Gao, X. & Thiemens, M. H. systematic study of sulfur isotopic composition in iron-meteorites and the occurrence of excess ^{33}S and ^{36}S . *Geochim. Cosmochim. Acta* **55**, 2671–2679 (1991).
- Farquhar, J., Savarino, J., Airieau, S. & Thiemens, M. H. Observation of wavelength-sensitive mass-independent sulfur isotope effects during SO_2 photolysis: Implications for the early atmosphere. *J. Geophys. Res.* **106**, 32829–32839 (2001).